THE ASTROPHYSICAL JOURNAL, 311:921–929, 1986 December 15

EXCITATION OF METHYL CYANIDE IN THE HOT CORE OF ORION

E. C. SUTTON,[1,2] GEOFFREY A. BLAKE,[2,3] R. GENZEL,[1,2] C. R. MASSON,[4] AND T. G. PHILLIPS[4]

Received 1986 March 24; accepted 1986 May 21

ABSTRACT

The excitation of CH_3CN in the hot core of Orion is examined using high-sensitivity observational data at 1.3 mm. Observed line fluxes are analyzed by means of multilevel statistical equilibrium (SE) calculations which incorporate current theoretical values of the collisional excitation rates. The analysis is applied to both optically thin models of the hot core region and models with significant optical depths.

Trapping is found to play a critical role in the excitation of CH_3CN. An optically thin analysis yields a kinetic temperature of 275 K and a cloud density of 2×10^6 cm^{-3}. Unequal column densities are deduced in this case for the two symmetry species: $N_A = 1.4 \times 10^{14}$ cm^{-2} and $N_E = 2.0 \times 10^{14}$ cm^{-2}, averaged over a 30″ beam. However, significant optical depths are expected if the hot core source is as small as 10″. Using this source size, line trapping noticeably modifies the emergent spectrum. It is possible, with this amount of trapping, to fit the data with equal amounts of the A and E symmetry species: $N_A = N_E = 2.3 \times 10^{14}$ cm^{-2}. The deduced cloud density and temperature are lowered to 1.5×10^6 cm^{-3} and 240 K. The model with trapping is favored because of the agreement with measured sizes of the hot core source and the more plausible N_A/N_E ratio.

Analysis of radiative excitation in the hot core indicates it is unlikely to significantly affect the ground vibrational state populations of CH_3CN. It most likely is significant for excitation of the v_8 band.

Subject headings: interstellar: molecules — nebulae: Orion Nebula — radiative transfer

I. INTRODUCTION

A large volume of literature presently exists which discusses excitation conditions in the "hot core" region of the Orion molecular cloud. This region is a component of the molecular gas which is kinematically distinct from the quiescent molecular cloud and is characterized by an average velocity of $v_{LSR} \approx 5$ km s^{-1} and a velocity dispersion of ~ 10 km s^{-1}. Excitation conditions in this material seem to require it to be rather dense ($n \approx 10^7$ cm^3) and with relatively high kinetic temperature ($T_k \approx 150$–250 K) (Morris, Palmer, and Zuckerman 1980; Genzel *et al.* 1982; Pauls *et al.* 1983).

Much of the observational literature on this region concerns the symmetric top molecule CH_3CN. Initially detected in Orion by Lovas *et al.* (1976), the excitation of methyl cyanide was first studied in detail by Loren, Mundy, and Erickson (1981). They concluded that the excitation temperature in this region was as high as 270 K, without, however, discussing directly the values of density and kinetic temperature needed to achieve this excitation. Goldsmith *et al.* (1983) observed vibrationally excited lines of CH_3CN (and HC_3N) and discussed a model based on radiative excitation. The most thorough analysis and the one drawing on the largest data set was that of Loren and Mundy (1984). They concluded that the hot core emission from methyl cyanide arose in a region with a density of 1–3×10^6 cm^{-3} and a kinetic temperature of $T_k = 275 \pm 25$ K. Most recently, however, Andersson, Askne, and Hjalmarson (1984) conclude that the density and temperature are much lower ($n \approx 10^{4.8}$ cm^{-3}, $T_k \approx 120$ K).

The interest in methyl cyanide is well founded. A symmetric top molecule shows emission in bands of lines covering a wide range in energy levels. Since these lines appear adjacent to each other in the spectrum, their relative calibration is well established. In addition, methyl cyanide is a heavy molecule so that many lines, involving large values of the quantum numbers J and K, may be observed. The dipole moment and the column density (in Orion) are large, so these lines are very strong. Selection rules generally allow radiative transitions only within K ladders, but collisional transitions are permitted across ladders as well. Comparison of transitions involving various values of J and K allows for some discrimination between the effects of density (which affects the rate of collisional transitions) and of temperature (which determines the likelihood of a large gain in rotational energy). While comparison of lines from different K ladders does not directly yield the kinetic temperature (as in the rotation diagram method), with enough different transitions available it is possible to arrive at relatively independent determinations of both density and temperature.

The analytical tools for such analyses were most fully developed by Cummins *et al.* (1983) and Loren and Mundy (1984). Radiative de-excitation is treatable within the large-velocity gradient formalism (Sobolev 1963; Castor 1970; Goldreich and Kwan 1974). Since the optical depths for methyl cyanide lines are generally small or modest, there can be only moderate trapping of the radiation and the photon escape probability is of order unity. State-to-state collisional transition rates are determined to good approximation by a method (Cummins *et al.* 1983) which relates them to a few fundamental collisional rates. On the basis of such a methodology, Loren and Mundy (1984) in effect determine populations of the various rotational levels and through them can reconstruct the observed line ratios.

Several matters prompt reexamination of the previous analyses of methyl cyanide excitation. First is the existence of new, higher sensitivity observational data (Sutton *et al.* 1985;

[1] Space Sciences Laboratory, University of California, Berkeley.
[2] Department of Physics, University of California, Berkeley.
[3] Department of Chemistry, University of California, Berkeley.
[4] Department of Physics, California Institute of Technology.

Blake *et al.* 1986). These observations have considerably better signal-to-noise ratios and extend the data to significantly higher energy levels. These higher energy transitions (including numerous excited vibrational state lines) are especially important in determining the effects of kinetic temperature. Second, there is the persistence of analyses arguing for significantly lower kinetic temperatures which need to be explained. A third reason is the recent availability of more accurate collisional rate data (Green 1986). And finally, there is the need to extend the analysis to include considerations of the relative populations of the A and E species, to include the effect of line opacity and trapping, and to include a more complete analysis of radiative pumping.

II. SPECTROSCOPY OF CH_3CN

The energy levels of a symmetric top, such as CH_3CN, are described by the quantum numbers J and K, where J is the total angular momentum and K is its projection on the symmetry axis. Since methyl cyanide is highly prolate, there is a large increase in energy with increased K. The energy of a rotational level, including centrifugal distortion, is given by

$$\frac{E(J, K)}{h} = BJ(J+1) - D_J J^2(J+1)^2 - D_{JK} J(J+1)K^2 + (A-B)K^2 - D_K K^4 , \quad (1)$$

where for methyl cyanide $B = 9198.9$ MHz, $A = 157300$ MHz, $D_J = 3.8 \times 10^{-3}$ MHz, $D_{JK} = 177 \times 10^{-3}$ MHz, and $D_K = 2.84$ MHz (Boucher *et al.* 1980). The hyperfine structure is negligible for the levels of interest here.

Methyl cyanide is of point group C_{3v}. The presence of the three identical hydrogen nuclei leads to a separation of the rotational levels into two symmetry species, distinguished by their nuclear spin state. Levels where K is a multiple of 3, $K = 0, 3, 6, \ldots$, belong to the A symmetry state while those with K not a multiple of 3, $K = 1, 2, 4, 5, \ldots$, belong to the E species. The A symmetry states have twice the spin statistical weight of the E states. These states are similar to the ortho- and para-forms of H_2 or NH_3. Since a transition between these forms requires a modification of a nuclear spin, the species interconvert only very slowly.

The lowest lying vibrational state is designated v_8 and corresponds roughly to a bending motion of the C-C-N bond. The vibrational energy is 364.71 cm^{-1} (Duncan *et al.* 1978), making it comparable in energy to some of the relatively low pure rotational levels. The vibrational motion is doubly degenerate, giving rise to an additional quantum number $l = \pm 1$, the vibrational angular momentum about the symmetry axis. For most purposes $K - l$ replaces the quantum number K from the ground vibrational state (where $l = 0$). There is a small splitting of the levels with different l. These effects are shown in the energy level diagram for CH_3CN (Fig. 1).

III. OBSERVATIONAL DATA

The observations analyzed here were obtained as part of the Owens Valley molecular line survey of OMC-1 between 215 and 247 GHz (Sutton *et al.* 1985) and its subsequent extension to the 247–263 GHz band (Blake *et al.* 1986). This frequency interval contains the $J = 12$–11, 13–12, and 14–13 bands of CH_3CN. The vibrational ground state transitions are seen out to a value of K as large as 10. For all three bands vibrationally excited transitions ($v_8 = 1$) are also seen, out to values of $K - l \approx 6$. The highest energy transitions in both ground and excited vibrational states are $\sim$800 K above the ground state.

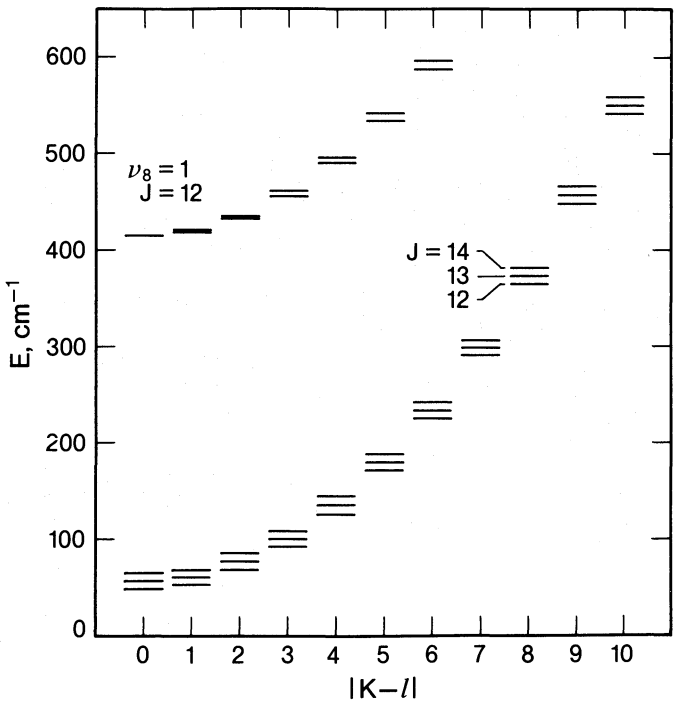

FIG. 1.—Energy level diagram for CH_3CN in the ground vibrational state and the first excited vibrational state (v_8). Only $J = 12$ levels are shown in the v_8 state, and the splitting for $K - l = 0$ has been suppressed.

The data for the three bands are summarized in Table 1. The integrated line strengths presented here differ from those quoted by Sutton *et al.* (1985) and Blake *et al.* (1986) in that the values for $K = 0$–5 are based on Gaussian decompositions of the lines into "spike" and "hot core" components. The line strengths shown are those of the hot core component. The maximum contribution from spike emission was $\sim$25% for $K = 0$. The spike emission is well modeled by LTE emission with $T_{ex} = 100$ K and $N_c \approx 7 \times 10^{13}$ cm^{-2}, so this deconvolution is thought to be fairly accurate. Since the $K = 0$ and $K = 1$ line frequencies are very close, their intensities are based on a further deconvolution of the blended hot core profiles, making these particular values somewhat uncertain. A further correction has been made for isotopic emission. The $K = 5$ and $K = 6$ ground-state lines are corrected for contributions from the $K = 0$, 1, and 3 lines of the $CH_3{}^{13}CN$ isotope, assuming an isotopic ratio of $[CH_3CN]/[CH_3{}^{13}CN] = 30$ and that all lines are optically thin. This ratio best fits the $K = 1$ and $K = 2$ isotopic lines, although it is different than the deduced ratio for the other isotopic species, $[CH_3CN]/[{}^{13}CH_3CN] \approx 12$, presumably because of chemical fractionation. But again, the correction is small ($<10\%$). The low isotopic ratios *do* suggest some degree of saturation in the CH_3CN lines, an effect which will be discussed below. The isotopic lines are not directly included in the analysis since so few are available and their relative intensities are too uncertain. Finally, a few CH_3CN lines are omitted from Table 1 because of coincidences with lines of other molecules.

Uncertainties in the data are dominated by systematic effects. Statistical errors are typically in the range 0.5–1.0 K km s^{-1}, which are insignificant except for the weakest lines. The dominant systematic uncertainty is in the overall calibration which is thought to be accurate to $\pm 15\%$. A large

TABLE 1

HOT CORE INTENSITIES

TRANSITION	$\int T_a^* dv$ (K km s^{-1}) $J = 12$–11	$J = 13$–12	$J = 14$–13
	$v_8 = 0$		
$K = 0$	28.3	30.8	31.4
$K = 1$	38.4	22.6	30.9
$K = 2$	39.1	29.5	34.4
$K = 3$	34.6	30.4	37.3
$K = 4$	16.3	23.5	22.4
$K = 5$	14.0	19.5	...
$K = 6$	21.4	14.1	19.5
$K = 7$	5.3	5.4	9.6
$K = 8$	2.9	5.8	5.0
$K = 9$	...	2.4	3.5
$K = 10$	..	...	3.6
	$v_8 = 1$		
$K = 0$, $l = 1$	3.0	5.0	...
$K = 1$, $l = 1$	10.9	5.8	5.0
	2.9	3.5	3.5
$K = 1$, $l = -1$	2.5	4.6	...
$K = 2$, $l = 1$	2.4	2.3	3.3
$K = 2$, $l = -1$	6.2	6.4	...
$K = 3$, $l = 1$	2.4	6.2	6.6
$K = 3$, $l = -1$	1.7	2.1	...
$K = 4$, $l = 1$	4.1	8.2	...
$K = 4$, $l = -1$	0.8	...	...
$K = 5$, $l = 1$	1.6	2.0	...
$K = 5$, $l = -1$	1.8	...	...
$K = 6$, $l = 1$	1.9	...	1.8

fraction of that calibration error may also be present in the interband calibration. Apart from calibration the principal systematic errors are associated with the deconvolutions. Such errors should be $\sim 10\%$ of the hot core line intensities and should be restricted chiefly to the $K = 0$, 1, and 2 lines.

IV. STATISTICAL EQUILIBRIUM CALCULATIONS

The technique of statistical equilibrium calculation of rotational level populations for symmetric top molecules was first developed by Cummins *et al.* (1983). In this technique, the individual level populations are determined by an equilibrium of radiative and collisional processes. The dominant radiative process is spontaneous emission, causing de-excitation of high-lying energy levels. In the case of optically thick radiation, stimulated processes are also important and cause trapping of the emitted photons. Collisional processes cause both upward and downward transitions and, in addition, obey different selection rules than the radiative transitions. Collisional rates, in general, have been somewhat poorly known, and estimated rather than measured rates are generally used in calculations. For particular values of density and kinetic temperature, an equilibrium (but not thermalized) set of energy-level populations can be calculated numerically for competition between the radiative and collisional processes. The equilibrium populations of the model can then be compared with the observed emission spectrum from the molecular cloud. This is the basic technique used by Loren and Mundy (1984) to calculate the excitation of CH_3CN in Orion. The calculations described here follow this same procedure. As a test of their numerical results, the calculational code has been redeveloped independently of Loren and Mundy. Good agreement is obtained with their published results. Here the calculations are applied to examination of the higher energy transitions and extended to aspects of the data not previously addressed.

The rate of spontaneous emission from the level J, K to J–1, K is given by

$$A_{J,J-1} = \frac{64\pi^4}{3h}\frac{\nu^3}{c^3}\frac{\mu^2}{2J+1}\frac{J^2-K^2}{J}, \quad (2)$$

where h is Planck's constant, ν is the frequency of the transition, and $\mu = 3.91$ Debye is the permanent dipole moment. The quantity $(J^2 - K^2)/J$ is the line strength $S(J, K)$. For values of $J = 14$ and $K = 0$, this gives a spontaneous emission rate of 0.0015 s^{-1}.

To first order the above are the only allowed spontaneous radiative transitions. However, for high-lying energy levels, centrifugal distortion can create a small dipole moment perpendicular to the symmetry axis of the molecule (Oka 1976). This dipole moment can give rise to weakly allowed transitions following the selection rules $\Delta J = \pm 1, 0$, $\Delta K = \pm 3$. The distortion induced dipole moment is calculable from the quantity $(\theta_x^{xx})_{\rm eff}$ which is of the order of 10^{-6} Debye for CH_3CN (Oka, private communication). Using this value, the rate of the spontaneous $J, K = 14, 9 \rightarrow 13, 6$ transition (for example) is $\sim 2 \times 10^{-8}$ s^{-1}, which is negligible compared with other rates present. Despite the rapid dependence of the emission rate for this process on the quantum numbers J and K ($\sim J^4$ and K^3 for $J \gg K$) the decay rate should remain reasonably small for all levels with significant populations. These $\Delta K = 3$ transitions are also a potential source of radiative excitation in the far-infrared. The radiation field in the Orion core peaks in the 100 μm region where a number of these transitions fall. However, the induced rates again seem too small to have much effect.

Collisional transitions are allowed with selection rules of $\Delta K = 3n$, for integer values of n. Unlike the radiative case, no restrictions exist on the value of ΔJ, and also unlike the radiative case the $\Delta K = \pm 3$ rates are of comparable magnitude to those with $\Delta K = 0$. Because of the relatively unrestrictive selection rules, a large number of mutual collisional rates must be calculated between the various J, K levels (significant populations can exist in levels up to $J \approx 30$ and $K \approx 15$). Fortunately, these rates are not all independent. As discussed by Goldflam, Green, and Kouri (1977) and Green (1979), in the infinite order sudden (IOS) approximation the collisional rates between arbitrary excited states can be expressed in terms of "fundamental" excitation rates out of the ground rotational state ($J = K = 0$). The interstate collision rates are given by

$$R(J, K \rightarrow J'K') = (2J'+1)\sum_L \begin{pmatrix} J' & L & J \\ K' & K-K' & -K \end{pmatrix}^2 Q(L, |K-K'|), \quad K' = 0, \quad (3)$$

$$R(J, K \rightarrow J'K') = (2J'+1)\sum_L \left[\begin{pmatrix} J' & L & J \\ K' & K-K' & -K \end{pmatrix}^2 Q(L, |K-K'|) + \begin{pmatrix} J' & L & J \\ -K' & K+K' & -K \end{pmatrix}^2 Q(L, K+K')\right], \quad K' \neq 0,$$

where the $Q(L, M)$ are the fundamental rates and

$$\begin{pmatrix} J' & L & J \\ K' & K-K' & -K \end{pmatrix}$$

is a 3-j symbol. This yields both upward and downward rates, but the upward rates then need to be multiplied by $e^{-(E'-E)/kT}$ to satisfy the requirements of detailed balance.

The fundamental rates $Q(L, M)$ for excitation of CH_3CN by collision with H_2 were estimated by Cummins *et al.* (1983) to fall between limiting cases they designated as "hard" and "soft" rates. Recently, Green (1986) has calculated collisional rates in the infinite order sudden (IOS) approximation. These rates are similar to the "soft" rates of Cummins *et al.*, but with significantly smaller values for the $\Delta K > 0$ collisions. Comparison with coupled states (CS) calculations (Green 1985) indicates these rates are fairly accurate. The values for $Q(L, M)$ adopted here are those for a kinetic temperature of 140 K. The temperature dependence of the $Q(L, M)$ is weak and is neglected.

The highest collisional rates are of the order of 4×10^{-10} cm^3 s^{-1}. For a cloud with a H_2 density of 10^6 cm^{-3} this gives individual interstate rates of $\sim 4 \times 10^{-4}$ s^{-1}, comparable in magnitude with the rates given for spontaneous emission. In general, collisional transitions will be more rapid than spontaneous emission for the lower rotational levels, while for the higher levels the A-coefficient will increase rapidly and overwhelm the collisional transitions.

The chief step in analyzing the observational data of Table 1 is to calculate the populations of the various J, K levels. The column densities of the two symmetry species (N_A and N_E) are first normalized to unity. These populations are then distributed (for computational convenience) among the J, K levels according to separate, initial thermal distributions. Levels up to $K = 21$ and $J = 25$ are included. For various values of kinetic temperature and density the actual state-to-state collisional rates are determined. The level populations are then allowed to evolve until equilibrium is reached.

The matrix of rotational level populations fully describes the excitation of CH_3CN in the molecular cloud. The populations of the levels of interest here are shown in Figure 2 for a variety of cloud models. The basic effects may be briefly summarized. First, kinetic temperature is the dominant factor determining to how large a value of the quantum number K the population extends. This is to be expected because of the rapid variation in energy with K and the fact that collisions are needed to cause $\Delta K \neq 0$ excitations. Second, for excitation high inside a K ladder, $J \gg K$, the density determines the rate at which population falls off for increases in J. For high enough density, populations in adjacent J levels are equal, except for degeneracy factors. As the density is lowered, the population begins to fall off at a value of J where the collisional rate begins to fall below the spontaneous emission rate.

The calculation discussed so far is appropriate to an optically thin, nonradiatively pumped case. We can readily see the approximate result. Since the $J = 12$–11, 13–12, and 14–13 bands are observed to have similar intensities, the density must be high, at least of the order of 10^6 cm^{-3}. Since emission is seen to large K, the temperature must be large, greater than 250 K. These conclusions will be made more precise in the following section on the model fits to the data.

V. MODEL FITS TO THE DATA

a) Optically Thin Models

The emission spectrum may be predicted directly from the populations in the various levels if the cloud is optically thin. The peak antenna temperature of a transition from J, K to J–1, K is given by

$$T_R(pk) = \frac{16\pi^3}{3}\left(\frac{\ln 2}{\pi}\right)^{1/2}\frac{\nu\mu^2}{k}\frac{S(J, K)}{2J+1}\frac{N_{J,K}}{\Delta V} \quad (4)$$

where a Gaussian line shape of width ΔV has been assumed. The line strength is

$$S(J, K) = \frac{J^2 - K^2}{J}. \quad (5)$$

The more fundamental, and easier to measure, quantity is the integrated line strength

$$\int T_b\, dv = \frac{8\pi^3\nu^2\mu^2}{3kc} N_{J,K}\frac{S(J, K)}{2J+1}. \quad (6)$$

Since the experimental data have been tabulated in terms of a line strength integrated over velocity, the appropriate formulation is

$$\int T_b\, dv = \frac{8\pi^3\nu\mu^2}{3k} N_{J,K}\frac{S(J, K)}{2J+1}, \quad (7)$$

which has the same functional form as the equation for $T_R(pk)$ (eq. [4]). Since only relative intensities are needed, except for the final calculation of column density, the numerical constants may be largely ignored.

The best fits to the observed spectra are given by a density of $n = 2^{+2}_{-1} \times 10^6$ cm^{-3} and a kinetic temperature of $T_k = 275 \pm 25$ K, assuming the cloud is optically thin and there is no radiative pumping. This density and temperature fit both the A and E species data and are in excellent agreement with the results of Loren and Mundy (1984). Derived beam-averaged column densities for the two species are $N_A = 1.4 \times 10^{14}$ cm^{-2} and $N_E = 2.0 \times 10^{14}$ cm^{-2}. Equal quantities of the two forms of methyl cyanide are not plausible within these simplified models of the molecular cloud. This conclusion will be discussed in more detail below. The total column density $N_A + N_E$ is lower than that reported by Sutton *et al.* (1985) and Blake *et al.* (1986). This is in part due to an error in the partition function used in those previous calculations and in part due to the fact that the SE calculation inherently yields a lower (and more realistic) column density than the rotation diagram technique. It should be noted that there is no need here for a separate calculation of a partition function since the populations of all levels are calculated together.

b) Models with Radiative Trapping

Radiative trapping may be included fairly readily in the calculations described above. It is necessary to specify independently the amount of trapping present. This may be done either by specifying a source size, a source-averaged column density, or the optical depth of any one transition. The rate of spontaneous emission from each level is modified by multiplying the A-coefficient by the photon escape probability β. This is determined in the usual way for a spherical geometry with a velocity field proportional to radius: $\beta = (1 - e^{-\tau})/\tau$, where τ is the

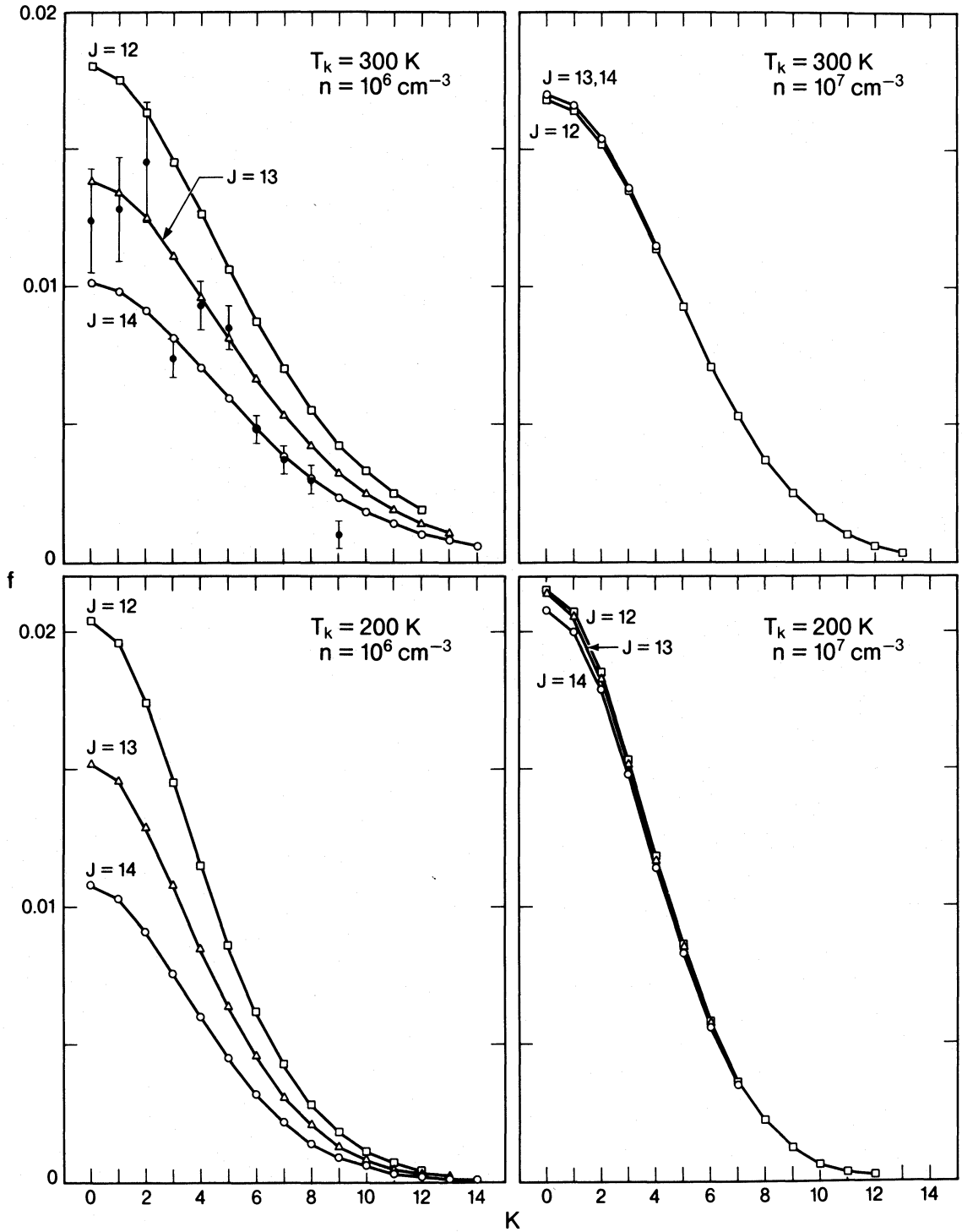

FIG. 2.—Fractional populations of (J, K) levels of CH_3CN for various optically thin cloud models. In each model the total populations of the A and E species have been separately normalized to unity. For convenience in plotting, the values for K = 3, 6, 9, and 12 have been divided by 2 to correct for the extra degeneracy of these levels. The data are plotted alongside the T_k = 300 K, $n = 10^6$ cm^{-3} model. For simplicity the data are presented as averages over the three bands. Differences between the bands are small, but show ~10% greater population for J = 12 and 10% less for J = 14. The best-fit model is intermediate to those shown. The K = 3 point is poorly fit by all optically thin models.

optical depth of the appropriate transition (de Jong, Chu, and Dalgarno 1975). The level populations are then allowed to evolve under the influence of collisions and the reduced spontaneous emission rate. The latter changes with time since τ and β evolve as the populations change. After the populations equilibrate, the emergent spectrum may be calculated as for the optically thin case, but with the fluxes reduced by the appropriate values of β.

The calculations here are based on a source size of 10″, consistent with the size for the hot core source determined by Masson *et al.* (1984, 1985) for CO and for hot dust emission and with the measured extent of the NH_3 emission (Pauls *et al.* 1983). This size is toward the upper end of the range originally suggested by Morris, Palmer, and Zuckerman (1980) for the ammonia source and significantly above the 3″–6″ sizes suggested by Goldsmith *et al.* (1982, 1983) for vibrationally excited HC_3N and CH_3CN. The trapping calculations described here give fairly similar results for source sizes ranging from 7″ to 14″.

The most significant change induced by trapping is a redistribution of population to higher J values. Ordinarily the excitation within a K ladder becomes strongly subthermal at levels where the spontaneous emission rate surpasses the collisional rates. To the extent that the effective spontaneous rate is reduced, the rotational relaxation will be less complete. The effect of trapping is similar to that of high densities since increased collisional rates also support populations of high J levels. An additional effect is associated with the spin degeneracy of methyl cyanide. Since the A species have twice the spin statistical weight of the E species, the highest optical depths and hence the highest amount of trapping occurs in the $K = 3$ ladder. This causes a reduction in the predicted fluxes of the $K = 3$ lines, mimicking a reduced column density of the A species. Finally, optical depths are higher in the low K lines, due to the larger populations, than for the higher K lines. The resulting saturation of the low energy (low K) lines mimics, in part, the effect of a higher kinetic temperature.

Level populations for these models with trapping are shown in Figure 3. The populations have been multiplied by the appropriate escape probabilities so the effects on the emergent spectrum may be directly seen. The smallest escape probabilities in these models are ~ 0.65. These values occur in the $K = 3$ ladder for J values in the range $J = 12$ to $J = 20$.

The best fit for a model with trapping and a 10″ source size is given by a density of $1.5^{+2}_{-0.5} \times 10^6$ cm^{-3} and a kinetic temperature of 240 ± 25 K. Since trapping reduces the flux in the $K = 3$ lines there is no longer need for different column densities for the A and E species. The derived beam-averaged column density is $N_A = N_E = 2.3 \times 10^{14}$ cm^{-2}.

c) *Models with Radiative Excitation*

The effects of radiative excitation may also be included in these models. The Orion molecular cloud contains within it strong sources of infrared radiation. In particular, IRc2 is thought to be the dominant energy source with a luminosity of $\sim 10^5\ L_\odot$ (Wynn-Williams *et al.* 1984). Its intrinsic spectrum is that of a blackbody at an effective temperature of ~ 700 K and with an effective source size of $\sim 1''$. Over a larger region this emission is degraded to longer wavelengths by dust heating and re-emission. This radiation field will affect molecular level populations in the surrounding molecular cloud through absorption and stimulated emission. Such processes can be important for both vibrational and rotational transition frequencies.

Although radiative excitation at the frequency of a molecular transition can not produce a net emission feature, it can affect the details of the emission spectrum. In general, microwave and millimeter-wave continuum emission will be ineffective at pumping the pure rotational transitions due to the declining dust opacity at long wavelengths. We estimate $\tau_d \approx 0.05$ at 1.3 mm in the hot core source. This is consistent with a peak column density of 10^{24} cm^{-2} for H_2 using the dust opacity values of Whitcomb *et al.* (1981) and a λ^{-1} dust opacity law. Assuming a dust temperature of 200 K, this is also consistent with the measured 2.6 mm flux and a ν^4 power law (Masson *et al.* 1985). If the radiation field in the hot core is isotropic thermal radiation at 200 K, this means that the rate of stimulated emission will be comparable to the spontaneous emission rate. Taken alone this seems like a large perturbation. But there will be a nearly equal rate in the opposite direction from absorption as long as the populations are comparable. The net effect is a small perturbation on the spontaneous emission. Since collisional rates dominate over spontaneous emission, particularly for the lower J levels, radiative pumping is expected to have only a minor influence on the molecular excitation. Detailed calculations with models including radiative excitation support this conclusion. This agrees with the result of Goldsmith *et al.* (1982) that radiative pumping will be ineffective at populating high J levels of the ground vibrational state. Since radiative and collisional rates within the first excited vibrational state are rather similar, this conclusion holds as well for excitation within the ν_8 state.

Excitation of the ν_8 vibrational mode at 365 cm^{-1} can be considered as a two-level problem using composite rates (collisional and radiative) into the various rotational sublevels. For the case of pure radiative pumping, the excitation temperature is independent of the value of the vibrational A-coefficient, being determined instead by the source temperature and geometrical dilution factors. Goldsmith *et al.* (1983) found that the excitation of the ν_8 mode could be explained by a model with pure radiative pumping. The vibrational excitation temperature measured here is 300 K, very similar to the inferred kinetic temperature, as expected if the gas is heated by close contact with the grains. Inclusion of collisional excitation and relaxation of the ν_8 level is difficult since it requires knowledge of the vibrational A-coefficient and cross sections for vibrational relaxation, both of which are rather poorly known. Using the estimates of Goldsmith *et al.* (1983) of $A_{\rm vib} = 4 \times 10^{-2}$ s^{-1} and $\langle \sigma v \rangle_{\rm vib} = 1.2 \times 10^{-12}$ cm^3 s^{-1}, it is unlikely that collisional processes can produce the observed excitation of the ν_8 mode, as discussed in § VI*a*. Using this estimate of the vibrational A-coefficient, it can be seen that the mechanism of Carroll and Goldsmith is also unlikely to be effective at populating high J levels of the ground vibrational state. This is due to the fact that the condition $n\gamma_{\rm rot} \ll A_{\rm rot}$ is not likely to be strongly enough satisfied to permit the multiple excitations required to populate high J levels.

VI. DISCUSSION: THE ORION HOT CORE

a) *Kinetic Temperature*

High kinetic temperature is one of the chief distinguishing features of the hot core region. The evidence for it was largely based on observations of nonmetastable inversion lines of NH_3 (Morris, Palmer, and Zuckerman 1980), from which the kinetic

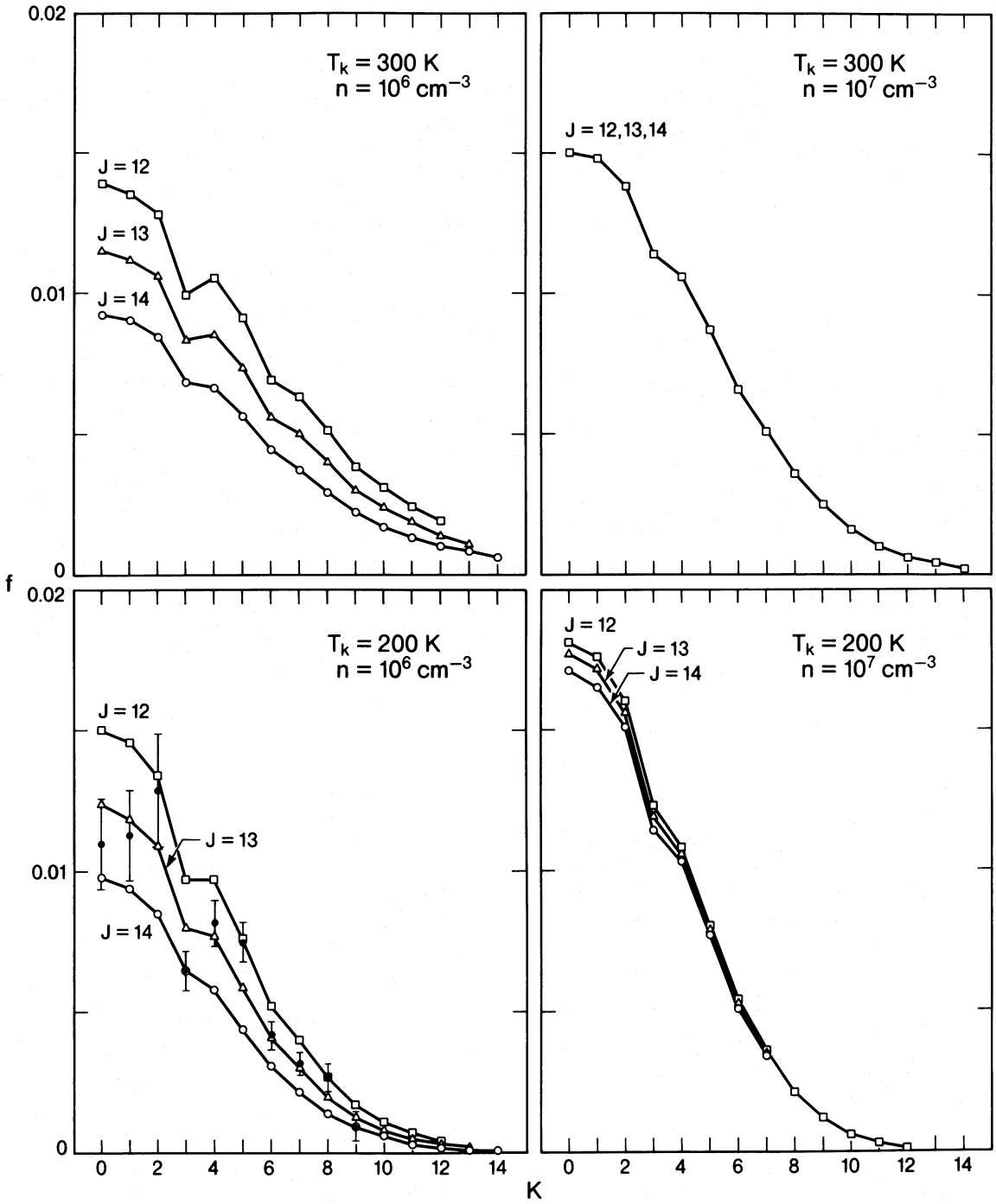

FIG. 3.—Fractional populations of (J, K) levels in CH_3CN multiplied by the escape probabilities for spontaneous emission. Optical depths are based on a 10″ source size. The values for K = 3, 6, 9, and 12 have been divided by 2. The data are plotted alongside the T_k = 200 K, n = 10^6 cm^{-3} model. The K = 3 point is reasonably well fitted by the models. The optical depth here is fixed by the assumed source size; somewhat better fits would be provided by modestly larger optical depths.

temperature was determined to be 220 K or greater. The work of Genzel *et al.* (1982) generally supported the conclusion of high kinetic temperature. Ziurys *et al.* (1981) obtained a rotation temperature of 150 K, based on high K metastable lines. Recent observations of optically thin metastable lines in $^{15}NH_3$ (Hermsen *et al.* 1985) have yielded lower rotational temperatures ($T_R \approx 110$ K). However, it is possible that these lower energy measurements were dominated by a cooler component of the hot core.

Rotational temperatures for a number of other molecules whose emission has a kinematic identification with the hot core has been typically ~150 K (C_2H_5CN, C_2H_3CN; Sutton *et al.* 1985; Blake *et al.* 1986). For methyl cyanide, the inferred kinetic temperature is larger, ~275 K (Loren and Mundy 1984). This difference has generally been interpreted as due to a concentration of the CH_3CN molecules in the hotter, denser parts of the region. Observations of low J lines of CH_3CN by Andersson, Askne, and Hjalmarson (1984) have suggested a

kinetic temperature of 120 K. These observations, however, were not sensitive to regions of high temperature since the energies of the levels involved were all less than 200 K. In addition, the low inferred temperature is closely coupled to a low density of $10^{4.8}$ cm^{-3}, invoked to explain apparent rotational relaxation of the $J = 6$ levels. Such a low density is inconsistent with collisional excitation of levels up to $J = 14$ as seen here. The other evidence for high excitation in the hot core is the observed vibrationally excited lines of HC_3N and CH_3CN (Goldsmith *et al.* 1982, 1983). However, the analysis of these lines is complicated by the possibility of radiative pumping of the vibrational transition.

For the data studied here it is simplest to start by considering just the high K (high-energy) ground vibrational state lines. These lines are primarily excited by collisions. Ordinary radiative selection rules do not permit direct radiative excitation. Rates via the $\Delta K = 3$ radiative transitions are too small. The mechanism of Carroll and Goldsmith (1981) of repetitive excitation to the $v_8 = 1$ state followed by decay back to the ground vibrational state works only for populating high J levels, not high K. The only mechanism other than pure collisions which might in principle work is one in which the collisional transfer is augmented by maintaining significant populations in high J ($J \approx 30$), low K levels through trapping or radiative pumping. However, this effect is not likely to be large and it still requires a significant kinetic temperature.

Since the most likely mechanism is population by collisions, the results of § V apply directly. For optically thin models, the best-fit kinetic temperature is $T_k = 275$ K. Models with trapping give somewhat lower temperatures ($T_k = 240$ K) for a 10″ source size. Kinetic temperatures less than 200 K can be fitted to the data but only for sources which are quite small ($\leq 7''$ diameter) and optically thick ($\tau \geq 2.5$).

Conversely, it can be asked whether there might be an even hotter component of the hot core gas. If there were hotter gas at, say, $T_k = 500$ K at densities sufficient to thermalize the observed levels ($n \approx 10^7$ cm^{-3}), the calculations show that the column density in this component would have to be less than 20% of that in the 275 K material, in order for the hotter gas not to dominate the high K spectrum. If the physical density were lower, the enhancement of the near metastable ($J \approx K$) high K levels would be even greater, and it would be difficult to get sufficient column density of such material. It is worth noting that hotter gas has been seen in Orion. The shocked gas seen in molecular hydrogen emission has a temperature of 2000 K (Beckwith *et al.* 1978). A cooler component of shocked material with $T \approx 750$ K and $N_{CO} \approx 3 \times 10^{17}$ cm^{-2} is responsible for far-IR emission from CO (Watson *et al.* 1980, 1985). However, this shocked material is kinematically distinct from that in the hot core and the column density is less than would be needed to be seen here.

Analysis of collisional excitation to the v_8 levels is difficult due to the lack of knowledge of collisional and radiative rate constants. Observationally, the populations of the v_8 levels are nearly the same as those of ground state levels of comparable energy. If the vibrational A-coefficient is 4×10^{-2} s^{-1} and the vibrational collision rate 1.2×10^{-12} cm^3 s^{-1}, as suggested by Goldsmith *et al.* (1983), the vibrational levels should be subthermally populated for $n \leq 10^{10}$ cm^{-3}. This suggests radiative excitation. Radiation can produce excitation temperatures near the kinetic temperature since the radiation is from warm dust grains which also heat the gas collisionally. Collisional excitation to the v_8 level could be plausible only if the vibrational A-coefficient were significantly smaller or the collision rate significantly larger. In any event, the argument for high kinetic temperature can be made independent of the analysis of vibrationally excited lines.

b) *Physical Density*

Much of the Orion molecular cloud, that in the "spike" or "ridge" component, is thought to exist at moderate densities of $n \approx 10^5$ cm^{-3}. Evidence for higher densities in the hot core material again is based on observations of NH_3 and a few other molecules. The nonmetastable NH_3 observations (Morris, Palmer, and Zuckerman 1980) suggested a minimum density of 5×10^7 cm^{-3} in the hot core. Townes *et al.* (1983) derived H_2 densities of $\sim 10^7$ cm^{-3}. In other molecules, CH_3CN observations have suggested densities of $\sim 10^6$ cm^{-3}. For excited vibrational states, even higher densities of 10^9 cm^{-3} or more are needed for models with pure collisional excitation, although radiative excitation models seem more likely (Goldsmith *et al.* 1982, 1983). In all of these cases the high densities are needed to maintain high collisional rates to the excited levels, in competition with high radiative decay rates.

In models with no trapping or pumping, at low values of K the calculated populations of the $J = 12$, 13, and 14 levels begin to diverge strongly for densities less than $\sim 10^6$ cm^{-3}. At this density the rate of collisions is insufficient to maintain the populations of these levels against spontaneous decay. Since the observed band intensities are nearly equal, this puts a good lower bound on the H_2 density. The upper limit is less well defined. Fully thermalized populations up to $K = 14$ are achieved at densities greater than 10^7 cm^{-3}. Although the best-fit distribution at $n = 2 \times 10^6$ cm^{-3} is somewhat subthermal, a fully thermalized distribution is also in reasonable agreement with the data.

Inclusion of trapping lowers the density required to keep the $J = 12$, 13, and 14 levels thermalized. For a 10″ source size, the best-fit density is 1.5×10^6 cm^{-3}. Again, significantly lower densities are implausible for this source size, but much higher densities can be tolerated.

c) N_A/N_E *Ratio*

Column densities for the A and E symmetry states of CH_3CN can be determined individually. The general expectation is that the ratio of these column densities should be near unity. The levels of the two species are comparable in energy and are interspersed. In addition, there are equal numbers of levels available, taking into account the extra spin degeneracy of the A species ($g_I(A) = 4$, $g_I(E) = 2$). If thermal equilibrium is established between the two species at temperatures of 50 K or greater, the populations of the two species will be very nearly equal. For equilibrium at very low temperature the A species will be more abundant because of the fact that the lowest energy state ($J, K = 0, 0$) is of the A symmetry. Equilibrium ratios for a range of temperatures are shown in Figure 4.

Despite this general expectation, there has been some evidence for nonequal abundances. In Sagittarius B2, Cummins *et al.* (1983) report a ratio of $N_A/N_E = 0.80$ for CH_3CN. The errors were unspecified but the fit was reported to be noticeably poorer with a ratio of unity. Goldsmith *et al.* (1983) mention a deficiency in the $K = 3$ intensity in the Orion hot core, also suggestive of an underabundance of the A species. Andersson *et al.* (1984) report a ratio in the other direction, $N_A/N_E \geq 1.1$. Loren and Mundy do not specifically discuss the

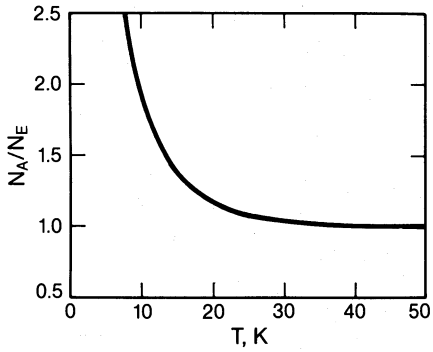

FIG. 4.—Equilibrium ratio of column densities for the A and E species of CH_3CN as a function of temperature.

A/E ratio, confining their analysis to the A symmetry species. However, their spectra suggest a ratio $N_A/N_E < 1$, the A lines being stronger than the adjacent E lines, but by less than the factor of 2 suggested by their statistical weights. This is the same result as obtained in the optically thin calculations described here where $N_A/N_E \approx 0.7$. This is particularly surprising since a ratio of less than unity is not explainable by any case of thermal equilibrium (Fig. 4).

Trapping provides a graceful solution to the problem of this unlikely result. The suggestion that $N_A < N_E$ is based chiefly on low fluxes in the $K = 3$ lines. Trapping is strongest in the $K = 3$ ladder because of the extra spin degeneracy of the A species. This is unlike the situation for $K = 0$ where this spin degeneracy is present but there is no K degeneracy. By $K = 6$ the populations are low enough that trapping is less significant. In the $K = 3$ ladder trapping works to reduce the emergent flux directly and also reduces populations in the individual levels by redistributing these populations to higher J. The combined result is to remove the requirement for $N_A < N_E$. This mechanism is most effective for models with $n \approx 1$–2×10^6 cm^{-3}. It should be emphasized that trapping is not artificially introduced to explain this anomalous ratio. It is independently required if the source size is of the order of 10″, consistent with other measurements.

VII. SUMMARY

Statistical equilibrium calculations provide information on molecular densities and kinetic temperatures. The CH_3CN emission in the hot core of Orion is a favorable case for such analysis because of its strong, well-calibrated, symmetric top spectrum. It has the disadvantage of being a molecule with a high dipole moment, giving high spontaneous emission rates and noticeable optical depths.

Models of optically thin emission yield cloud densities of $2^{+2}_{-1} \times 10^6$ cm^{-3} and kinetic temperatures of 275 ± 25 K. The latter is fairly tightly constrained, but the density determination is relatively loose, particularly on the upper side. In the optically thin case it is necessary to postulate different column densities for the two symmetry species in order to fit the data satisfactorily. The required beam-averaged column densities are $N_A = 1.4 \times 10^{14}$ cm^{-2} and $N_E = 2.0 \times 10^{14}$ cm^{-2}. A ratio of $N_A/N_E < 1$ is difficult to explain; equilibration of the two species always gives $N_A/N_E \geq 1$. Above ~50 K, the equilibrium ratio should be very close to unity.

For optical depths approaching unity, trapping provides a significant perturbation to the spectrum. The effects are largest for $K = 3$ and act to increase the calculated ratio N_A/N_E. Significant optical depths are independently justified by measurements of the hot core source size. For a source size of 10″, equal values of N_A and N_E are possible. The best fit under these conditions is $n = 1.5 \times 10^6$ cm^{-3}, $T_k = 240 \pm 25$ K, and $N_A = N_E = 2.3 \times 10^{14}$ cm^{-2}.

The authors are grateful to S. Green for his communication of collisional rate data prior to publication. One of us (G. A. B.) acknowledges financial support from the Miller Research Institute.

REFERENCES

Anderson, M., Askne, J., and Hjalmarson, A. 1984, *Astr. Ap.*, **136**, 243.
Beckwith, S., Persson, S. E., Neugebauer, G., and Becklin, E. E. 1978, *Ap. J.*, **223**, 464.
Blake, G. A., Sutton, E. C., Masson, C. R., and Phillips, T. G. 1986, *Ap. J. Suppl.*, **60**, 357.
Boucher, D., Burie, J., Bauer, A., Dubrulle, A., and Demaison, J. 1980, *J. Phys. Chem. Ref. Data*, **9**, 659.
Carroll, T. J., and Goldsmith, P. F. 1981, *Ap. J.*, **245**, 891.
Castor, J. I. 1970, *M.N.R.A.S.*, **149**, 111.
Cummins, S. E., Green, S., Thaddeus, P., and Linke, R. A. 1983, *Ap. J.*, **266**, 331.
de Jong, T., Chu, S.-I., and Dalgarno, A. 1975, *Ap. J.*, **199**, 69.
Duncan, J. L., McKean, D. C., Tullini, F., Nivellini, G. D., and Pena, J. P. 1978, *J. Molec. Spec.*, **69**, 123.
Genzel, R., Downes, D., Ho, P. T. P., and Bieging, J. 1982, *Ap. J. (Letters)*, **259**, L103.
Goldflam, R., Green, S., and Kouri, D. J. 1977, *J. Chem. Phys.*, **67**, 4149.
Goldreich, P., and Kwan, J. 1974, *Ap. J.*, **189**, 441.
Goldsmith, P. F., Krotkov, R., Snell, R. L., Brown, R. D., and Godfrey, P. 1983, *Ap. J.*, **274**, 184.
Goldsmith, P. F., Snell, R. L., Deguchi, S., Krotkov, R., and Linke, R. A. 1982, *Ap. J.*, **260**, 147.
Green, S. 1979, *J. Chem. Phys.*, **70**, 816.
———. 1985, *J. Phys. Chem.*, **89**, 5289.
———. 1986, *A.J.*, **309**, 309.
Hermsen, W., Wilson, T. L., Walmsley, C. M., and Batrla, W. 1985, *Astr. Ap.*, **146**, 134.
Loren, R. B., and Mundy, L. G. 1984, *Ap. J.*, **286**, 232.
Loren, R. B., Mundy, L. G., and Erickson, N. R. 1981, *Ap. J.*, **250**, 573.
Lovas, F. J., Johnson, D. R., Buhl, D., and Snyder, L. E. 1976, *Ap. J.*, **209**, 770.
Masson, C. R., *et al.* 1984, *Ap. J. (Letters)*, **283**, L37.
Masson, C. R., Claussen, M. J., Lo, K. Y., Moffet, A. T., Phillips, T. G., Sargent, A. I., Scott, S. L., and Scoville, N. Z. 1985, *Ap. J. (Letters)*, **295**, L47.
Morris, M., Palmer, P., and Zuckerman, B. 1980, *Ap. J.*, **237**, 1.
Oka, T. 1976, in *Molecular Spectroscopy: Modern Research*, Vol. **2**, ed. K. N. Rao (New York: Academic Press), p. 229.
Pauls, T. A., Wilson, T. L., Bieging, J. H., and Martin, R. N. 1983, *Astr. Ap.*, **124**, 23.
Sobolev, V. V. 1963, *A Treatise on Radiative Transfer* (Princeton: Van Nostrand).
Sutton, E. C., Blake, G. A., Masson, C. R., and Phillips, T. G. 1985, *Ap. J. Suppl.*, **58**, 341.
Townes, C. H., Genzel, R., Watson, D. M., and Storey, J. W. V. 1983, *Ap. J. (Letters)*, **269**, L11.
Watson, D. M., Genzel, R., Townes, C. H., and Storey, J. W. V. 1985, *Ap. J.*, **298**, 316.
Watson, D. M., Storey, J. W. V., Townes, C. H., Haller, E. E., and Hansen, W. L. 1980, *Ap. J. (Letters)*, **239**, L129.
Whitcomb, S. E., Gatley, I., Hildebrand, R. H., Keene, J., Sellgren, K., and Werner, M. W. 1981, *Ap. J.*, **246**, 416.
Wynn-Williams, C. G., Genzel, R., Becklin, E. E., and Downes, D. 1984, *Ap. J.*, **281**, 172.
Ziurys, L. M., Martin, R. N., Pauls, T. A., and Wilson, T. L. 1981, *Astr. Ap.*, **104**, 288.

GEOFFREY A. BLAKE, R. GENZEL, and E. C. SUTTON: Space Sciences Laboratory, University of California, Berkeley, CA 94720

C. R. MASSON: Downs Laboratory of Physics, 405–47, California Institute of Technology, Pasadena, CA 91125

T. G. PHILLIPS: Downs Laboratory of Physics, 320-47, California Institute of Technology, Pasadena, CA 91125